



Compact Wideband/Dual band Antenna Structure based Semicircular DGS for WIFI and Sub-6 GHz 5G Wireless Applications

Rania Hamdy Elabd^{1,4}, Marwa E. Mousa¹, Amr H. Hussien², Amany A. Megahed¹, and Ahmed A. Kabeel³

¹Electronic and Communication Dept., Higher Institute of Engineering and Technology in New Damietta, Damietta 34517, Egypt

²Electronics and Electrical Communications Engineering Dept., Faculty of Engineering, Tanta University, Tanta 31527, Egypt.

³Electronics and Communications Engineering Dept., Faculty of Engineering, Delta University Egypt, New Damietta, Egypt.

⁴Electronics and Communications Engineering Dept., Faculty of Engineering, Horus University, New Damietta, Egypt.

Corresponding author: Rania Hamdy Elabd, Eng.rania87@yahoo.com, rania.hamdy@ndeti.edu.eg

Abstract- This work presents the design and construction of a ground plane semicircular slot based on planar antennas for wideband applications, including sub-6 GHz 5G wireless and WiFi. The radiating patch is designed to have a U shape with a transmission line feed. Beneath the radiating patch, a semicircle-Defected Ground Structure (DGS) is carved to control the bandwidth and minimize the size of the antenna. A two T-shaped stub construction one on the top of the other is affixed in the center of the U-shaped radiating area to enable wideband operation. The antenna functions as a Wide-Band Antenna (WBA) if the width of transverse portion of the top T construction is equal to the width of U shape. Additionally, shortening and altering the transverse sector of the upper T structure is equal to creating a band-stop filter with an adjustable resonant frequency that regulates the antenna's two operational bands. The design has a small footprint of $(0.35\lambda_0 \times 0.35\lambda_0)$ where λ_0 denotes the free space wavelength, peak gain, and efficiency of about 6.1 dBi and 93%, respectively. When the length of the top T-shape $W_{f2} = 27 \text{ mm}$, the antenna acts as a WBA with frequency band from 2.07 GHz to 5.8 GHz. Moreover, a time-domain analysis highlights the antenna's responsiveness and adaptability to wireless applications by providing insightful information on how it reacts to transitory signals

Keywords- Defected ground structure (DGS), Wideband antenna (WBA), WiFi, and 5G Communications.

1. Introduction

Worldwide, cellular mobile telecommunications services are becoming more and more prevalent. People often use their cell phones in close proximity to their heads. The ever-growing proliferation of wireless mobile services has forced mobile phone manufacturers all around the world to consider the interactions between mobile terminals and human bodies. On the one hand, some of the electromagnetic wave that the antenna generates is absorbed by the human skull. However, the presence of a human head alters a number of characteristics related to mobile phone antennas, including radiation efficiency, bandwidth, return loss, and radiation pattern. The relationship between the human head and the antenna has been studied by a number of academics.

For fifth-generation (5G) connection, the majority of research societies are concentrating on obtaining high throughput and high data rates at a cheap cost. The anticipated data rate for fifth-generation (5G) communication systems is 1000 times faster than that of fourth-generation (4G) communication systems (U. Rafique 2022). The Radio Access Networks (RANs) for 5G are anticipated to manage numerous 5G bands concurrently, in addition to handling a range of frequencies (S. M. Asif 2019). So as to assess the request for the spectrum essential for

International Mobile Telephony (IMT), the ITU-R has defined a number of metrics. Nearly all of the research required to achieve this demand's 2020 requirement has just been completed by ITU-R (S. Sarkar 2018).

The 5G frequency bands ITU n77 (3.3-4.2 GHz), n79 (4.4-5 GHz) and WIFI frequency (2.4 GHz) are covered by the proposed antenna. Based on thorough study, it is anticipated that the lower range of frequencies would provide significantly improved coverage for contemporary wireless communications. 5G communication would be able to deliver higher data speeds and broader coverage regions by outside-to-inside network coverage via frequency bands lower than 6 GHz (Elabd R.H. 2020). Many sub-6 GHz antenna designs that have been documented in the literature and shown to work well make considerable use of the printed antenna technology.

Thanks to technological advancements, antennas may now be smaller and more effective. A large fraction of this type of antennas are printed microstrip slot antennas (L. Dang 2010). Slot antennas have several applications, including WiMAX, WLAN, Bluetooth, 4G LTE, and others. Despite the apps that have already been released, slot antennas are extensively intended for wireless 5G applications, which mostly involve mobile terminal devices at the moment. The recommended rectangular slot antenna's design has been primarily focused on sub-6 GHz 5G applications for mobile portable devices.

Numerous methods for designing slot antennas have been documented in the literature. These include the following: a transformer triple band slot antenna (L. Dang 2010), a wideband slot antenna with fictitious resonances (X. Dong 2014) a hexagonal shaped slot antenna with U-shaped slot and two split rings (W. Hu 2019), a C-shaped coupled fed antenna with L-shaped monopole slot having orthogonal polarization (M. Li 2012), an octagonal shaped slot antenna with U-shaped strips for UWB applications (M. Bod 2012), a monopole radiator with square slot having L-shaped strips (W. Hu 2011), a monopole radiator with square slot having L-shaped strips (X. Dong 2014), a hexagonal shaped slot antenna with U-shaped slot and two split rings (W. Hu 2019), and inverted F-antennas for dual mode operation (A.K. Gautam 2016), a fractured-slotted ground plane with F-shaped structures (R. Khan 2018), an F-shaped slotted MIMO antenna with users hand effect (Elabd R. H. 2019), two monopole antennas with two rectangular etched slots and a T-shaped stub (W.C. Mok 2013), an elliptical patch antenna with an elliptical slot and dipole fed (R. Pandeewari. 2018), an antenna with a radiating element composed of Complementary Square Ring Resonator (CSRR) slots and fed by a meandered CPW (H. Alsaif 2018), U-shaped slot antennas with wide band applications (K.F. Lee 2008), (I.R.R. Barani, 2019).

The comparatively high gain, improved efficiencies, and small footprint of printed slot antenna designs, however, continue to be an issue. The literature lists a few drawbacks of slot antennas for 5G applications in the sub-6 GHz range, including their bigger slot size, narrow impedance bandwidth, low gain, low efficiency, etc. The antenna must be installed in conjunction with the mobile device's dielectric back cover because space is at a premium in 5G portable devices. Low profile antennas are necessary for 5G applications because of this. According to this, the entire antenna thickness at 3.3 GHz should be around 1mm (ANSI. 2006), (Ahlbom 1998) and (N.W. Liu, 2018). This study presents the design and implementation of semicircular slots in ground planes based on wideband and dual-band planar antennas for 5G and sub-6 GHz WiFi applications. A transmission line supplies power to the U-shaped radiating patch. The antenna's size may be decreased and the bandwidth can be adjusted thanks to a semicircle DGS that is engraved beneath the radiating patch. To enable wideband operation, the U-shaped radiating zone includes two T-shaped stub structures joined in the middle, one on top of the other.

When the length of transverse part of the upper T structure is equal U's limbs, the antenna becomes a WBA. A band-stop filter with a controllable resonant frequency can be additionally made by shortening and adjusting the length W_{f1} of the transverse sector of the lower T structure, which creates and controls the antenna's two operational bands. When $W_{f2} = 27 \text{ mm}$, the antenna act as WBA with frequency band from **2.07 GHz to 5.8 GHz**. When $W_{f1} = 8.6 \text{ mm}$, the antenna generates dual bands from **1.9 GHz to 3.7 GHz** and from **4.08 GHz to 5.6 GHz**. The antenna design has a compact size of $(0.35\lambda_0 \times 0.35\lambda_0)$ where λ_0 denotes the free space wavelength, peak gain, and efficiency of about **6.1 dBi** and **93%**, respectively. Excellent agreement is found between the observations and models.

The structure of the paper is as follows: The suggested antenna's design and simulation are explained in Methods and Experiment in Section 2, which makes use of the computer-simulated technology (CST) microwave package. Result and discussion are provided in Section 3. An analysis of the antenna's performance in the time domain is presented in Section 4. A comparison of the suggested antennas with the relevant works is shown in Section 5. Section 6 provides the conclusion at the end.

2. Methods and Experiment

In this section, highly efficient and compact designs for wideband and dual band antenna structures are introduced. The proposed antenna structures based semicircular slot DGS are designed on an FR4 substrate of thickness ($h =$

1.6 mm), dielectric constant/relative permittivity ($\epsilon_r = 4.5$), and the loss tangent ($\delta = 0.025$). The radiating patch is designed to have a U shape structure with a transmission line feed having a width W_f . Beneath the radiating patch, a semicircle DGS is carved to control the bandwidth and minimize the size of the antenna. A two T-shaped stub construction one on the top of the other is affixed in the center of the U-shaped radiating area to enable dual-band operation. Shortening and altering the transverse sector of the lower T structure is equal to creating a band-stop filter with an adjustable resonant frequency that regulates the antenna's two operational bands. Additionally, The antenna functions as a wideband antenna (WBA) if the width of transverse portion of the top T construction is equal to the width of U shape as shown in Figure 1 (a) and Figure 1 (b). The dimensions of the two proposed antenna structures are as listed in Table 1.

Figure 2 shows the simulated scattering parameter $|S_{11}|$ of the proposed antenna structure at various values of the parameters W_{f1} from 8.6 mm to 27 mm and W_{f2} from 8.6 mm to 27 mm. When the length W_{f1} of lower T- shaped structure varies from 8.6 mm to 27 mm the antenna functions as a dual band antenna. $W_{f1} = 8.6\text{mm}$ gives two operating bands 1.9 GHz to 3.7 GHz and from 4.08 GHz to 5.6 GHz, which makes the antenna viable for WIFI and sub-6 GHz 5G applications. The lower T-shaped structure with the length $W_{f1} = 8.6\text{mm}$ acts as a band-stop filter with a resonance frequency of 3.85 GHz. At this frequency, the return loss of the antenna is increased above $|S_{11}| > -10\text{ dB}$ and suppresses the frequencies from 3.7 GHz to 4.08 GHz. When the length of upper T- shaped structure $W_{f2} = 27\text{mm}$, the antenna functions as a WBA with a broad operating frequency band from 2.07 GHz to 5.8 GHz as shown in Figure 3 considering that $|S_{11}| \leq -10\text{ dB}$, which makes the antenna viable for WIFI and sub-6 GHz 5G applications.

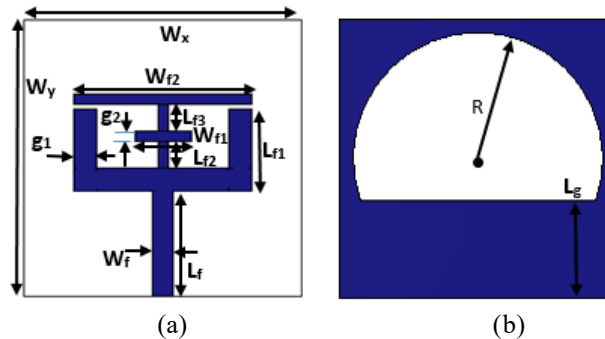


Fig. 1. Antenna structure (a) Top view and (b) Bottom view.

Table 1. The dimensions of the proposed antenna structures for both wideband and dual-band modes of operation.

| Parameter | Value (mm) | Parameter | Value (mm) |
|-----------|------------|-----------|------------|
| W_x | 42 | W_{f1} | 8.6 |
| W_y | 42 | W_{f2} | 27 |
| W_f | 3.172 | g_1 | 3.5 |
| L_f | 16 | g_2 | 1.6 |
| L_{f1} | 12.5 | L_g | 14.67 |
| L_{f2} | 4 | R | 19 |
| L_{f3} | 4 | | |

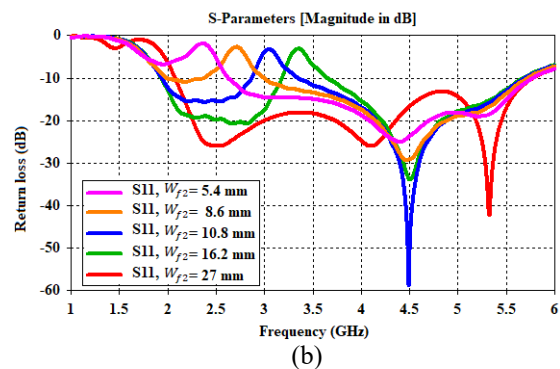
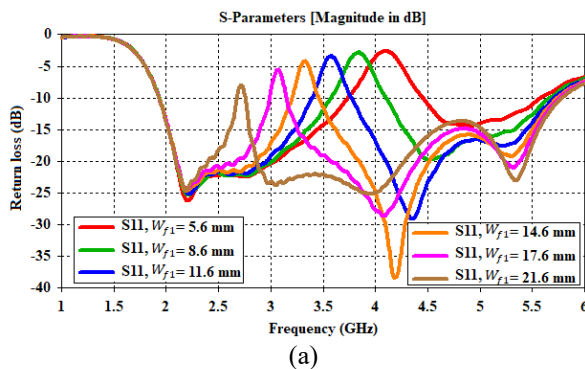


Fig. 2. The simulated scattering parameter $|S_{11}|$ of the proposed antenna structure at various values of the parameter W_{f1} and W_{f2} from 8.6 mm to 27 mm.

For a better understanding of how the proposal works, the surface current distributions are takeout and shown in Figure 4. The surface currents are abundant at the center T-shaped structure at 2.4 GHz , 4.5 GHz and flow along the double-folded edge of the feed patch at 3.3 GHz, respectively, forming wide frequency bands from 2.07 GHz to 5.8 GHz. With the assistance of the surface currents, wide frequency bands were created.

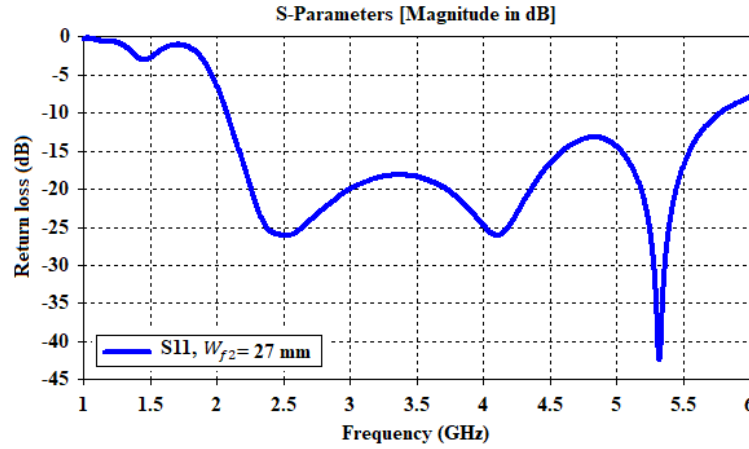


Fig. 3. Simulated return loss $|S_{11}|$ of the proposed antenna at $W_{f2} = 27$ mm.

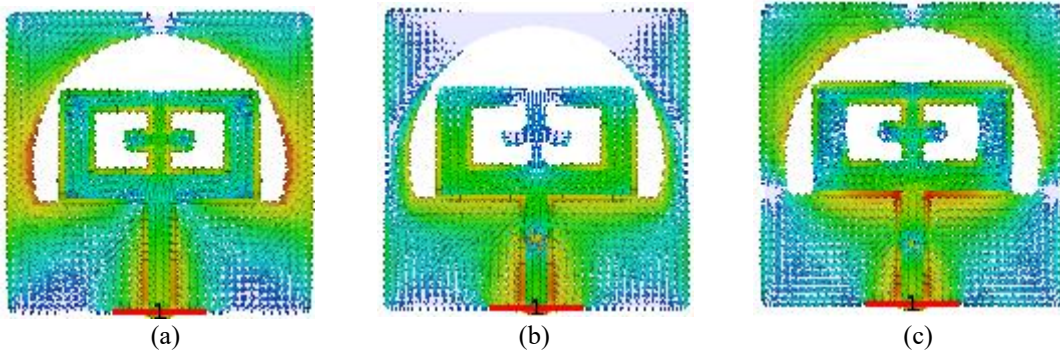


Fig. 4. Simulated current distributions at (a) 2.4 GHz, (b) 3.3 GHz and (b) 4.5 GHz.

3. Result and discussion

The photo etching procedure is used to fabricate the proposed antennas prototypes as shown in Figure 5 (a) and Figure 5 (b). The antenna measurement set-up, which comprises a Vector Network Analyzer (VNA-E5071C) and a test measurement horn antenna configuration in an anechoic chamber, is used to characterize the manufactured prototypes and calculate the radiation parameters in the azimuth and elevation planes.

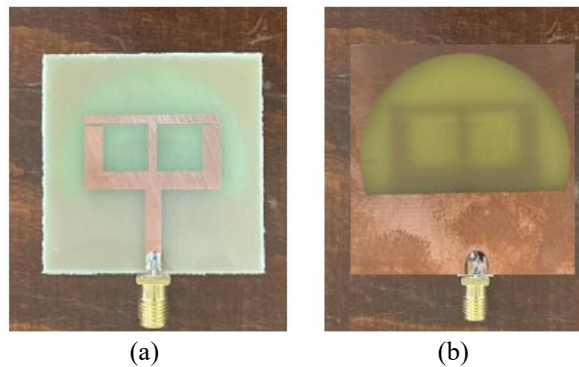


Fig. 5. Fabricated prototypes of the proposed antennas. (a) Top view and (b) Bottom view.

The comparisons between the simulated and measured return losses of the proposed antenna prototypes for $W_{f_2} = 27 \text{ mm}$ are shown in Figure 6. The measurements revealed that the antenna resonates in the frequency range from 2.15 GHz to 5.9 GHz that covers the WIFI frequency (2.4 GHz), sub-6 GHz frequency bands $n77$ ($3.3 - 4.2 \text{ GHz}$), $n78$ ($3.3 - 3.8 \text{ GHz}$), and $n79$ ($4.4 - 5 \text{ GHz}$) that are defined by ITU for next-generation 5G applications [15].

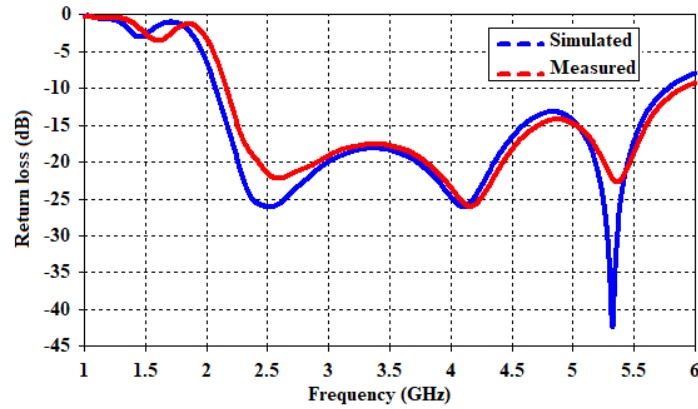
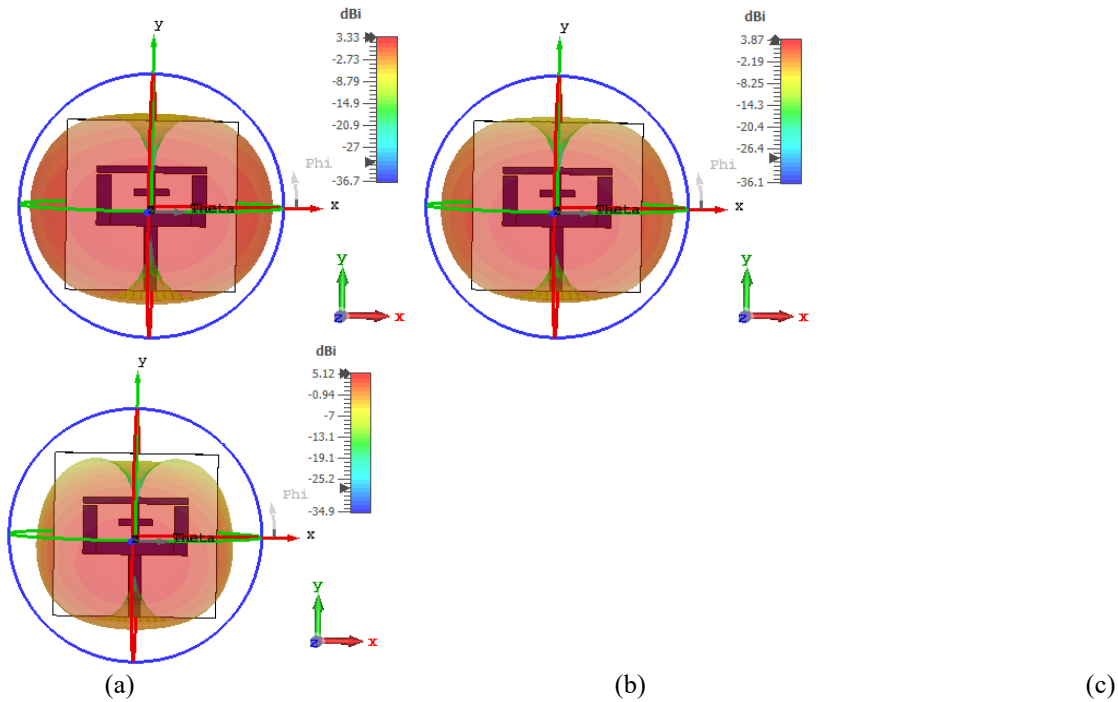


Fig. 6. Measured and simulated return loss of the proposed antenna.

Figure 7 depicts the simulated 3D radiation patterns and the simulated and measured 2D radiation patterns of the proposed antenna for $W_{f_2} = 27 \text{ mm}$ at the desired frequencies of 2.4 GHz , 3.3 GHz and 4.5 GHz . Co-polarization and cross-polarization plots are presented in the radiation pattern in both the E-plane and H-plane.



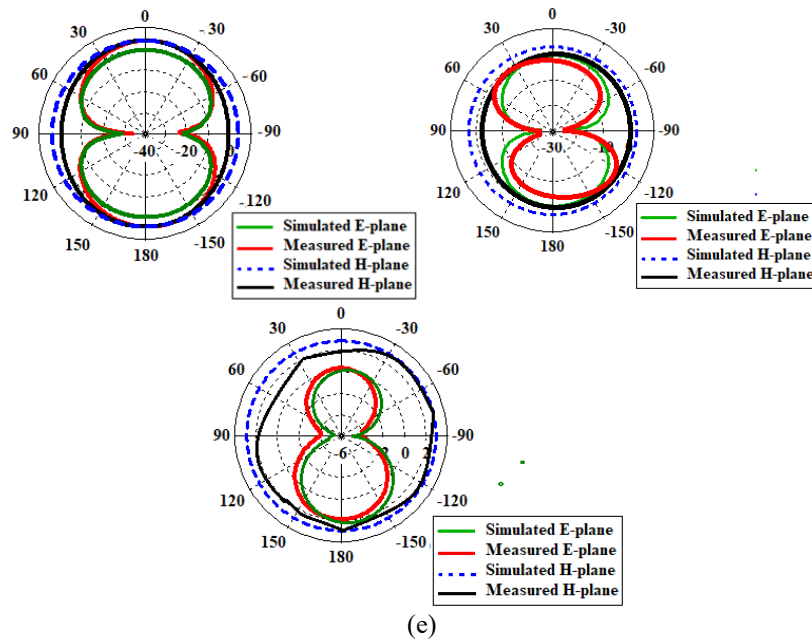


Fig. 7. The 3D radiation patterns of the proposed antenna for $W_{f2} = 27 \text{ mm}$ at: (a) 2.4 GHz, (b) 3.3 GHz and (c) 4.5 GHz, and the measured and simulated 2D radiation patterns of the proposed antenna for $W_{f2} = 27 \text{ mm}$ at: (d) 2.4 GHz, (e) 3.3 GHz, and (f) 4.5 GHz.

It is clear that the measured and simulated patterns are highly matched. The small differences between the measured and simulated results might be the consequence of inaccuracies committed in the manufacturing and soldering of the connectors. In addition, the anechoic chamber's settings, which may have additional metal, contribute to the changes in the measured S-parameters and radiation patterns.

The Gain Transfer Method/Gain Comparison Method has been used to evaluate the gain of the proposed antenna design in accordance with the IEEE standard test procedure. The gain computation uses a single reference antenna that is placed on an antenna positioner within the anechoic chamber and has a known gain. After that, the built prototype is oriented to face the direction of maximum radiation and to run parallel to the reference horn antenna. In order to calculate the gain of the proposed antenna in relation to the reference antenna, we activated the S_{21} parameter during the measurement procedure using the VNA.

According to the observed data, for $W_{f2} = 27 \text{ mm}$, the proposed antenna's realized peak gain is 8 dBi, which is consistent with the peak gain calculated by the simulation displayed in Figure 8 of about 6.2 dBi.

Since all antenna measurement equipment is automated, the gain is determined prior to the directivity and reflection coefficient. The antenna's efficiency is computed last. According to the observed data, the constructed prototype radiates at a total efficiency of around 90%, which is similar to the outcomes of the simulations displayed in Figure 9.

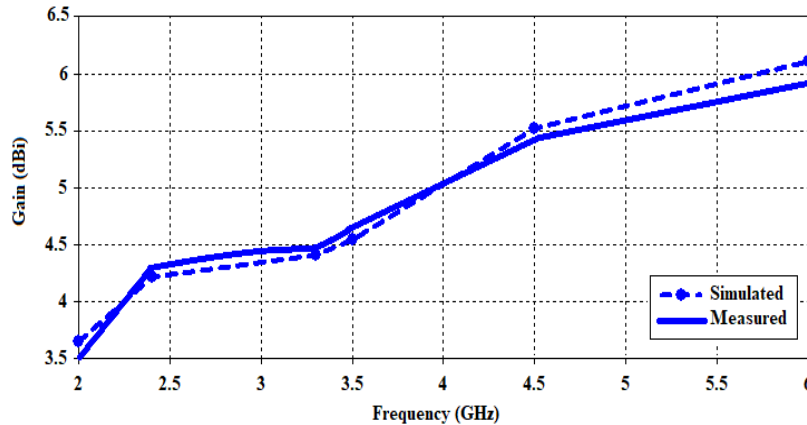


Fig. 8. Gain of the proposed antenna.

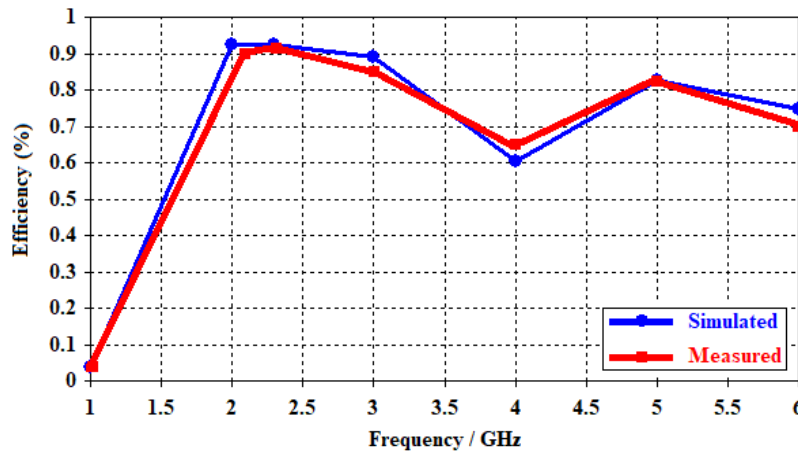


Fig. 9. Efficiency of the proposed antenna.

4. Analysis of the Antenna's Performance in the Time Domain

The antenna's time-domain performance is studied in detail, including group delay, S_{21} phase, and forward transmission coefficient (S_{21}). The simulated time-domain configuration is shown in three different settings (face-to-face, face-to-side, and side-to-side) in Figure 10. Two identical antennas are placed in each of these arrangements 210 mm apart, or 2.5 times the wavelength (λ_0) at 3.5 GHz. In these configurations, one antenna functions as the transmitter (Tx) and the other as the receiver (Rx). The group delay, S_{21} phases, and S_{21} magnitudes are displayed in Figure 10. Figure 11 (a) makes it evident that the side-to-side antenna design has an S_{21} value over -30 dB at 2.4 GHz and reach to -40 dB at 4.5 GHz, whereas the face-to-face and side-to-face antenna configurations have an S_{21} value below -20 dB at 2.4 GHz, lower than -30 at 3.3 GHz, and 4.5 GHz.

In Figure 11 (b), the S_{21} phase is also displayed to help understand the linearity characteristics within the intended band operation. It is clear from the phase curves that the antenna behaves linearly in the desired frequency range in a variety of orientations. Figure 11 (c) presents the group delay results to support this observation. At 2.4 GHz, the group delay is around 0.5 ns, while at 3.3 GHz and 4.5 GHz, it is roughly 0.4 ns.

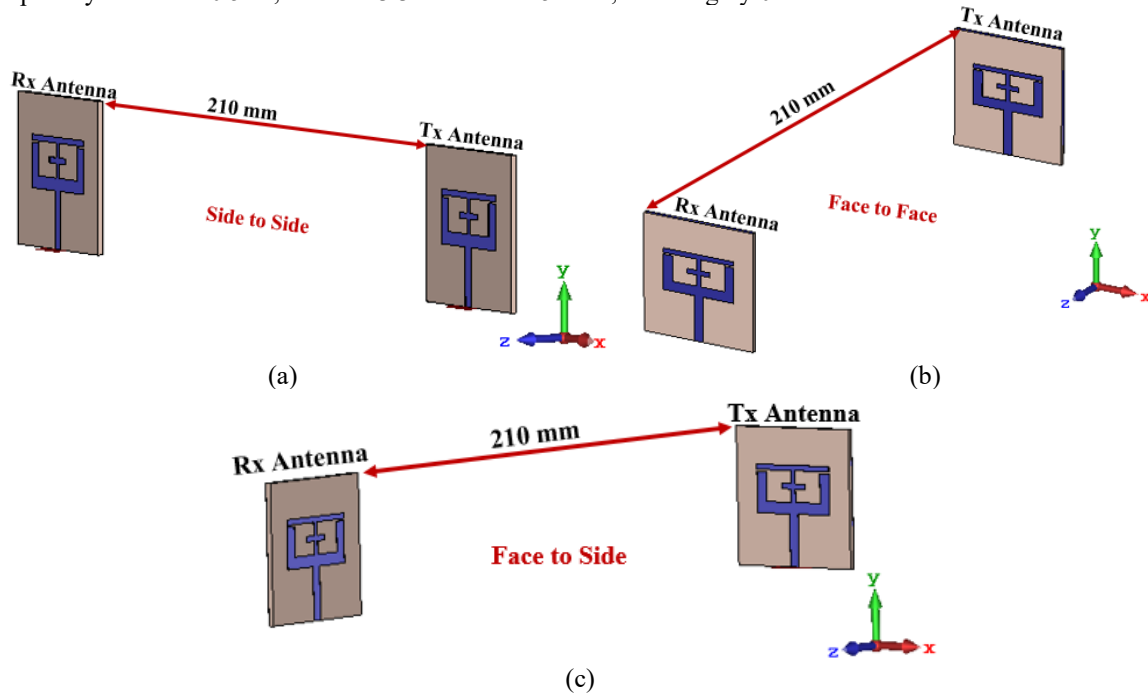


Fig. 10. Setup for time-domain analysis in simulations with various configurations.

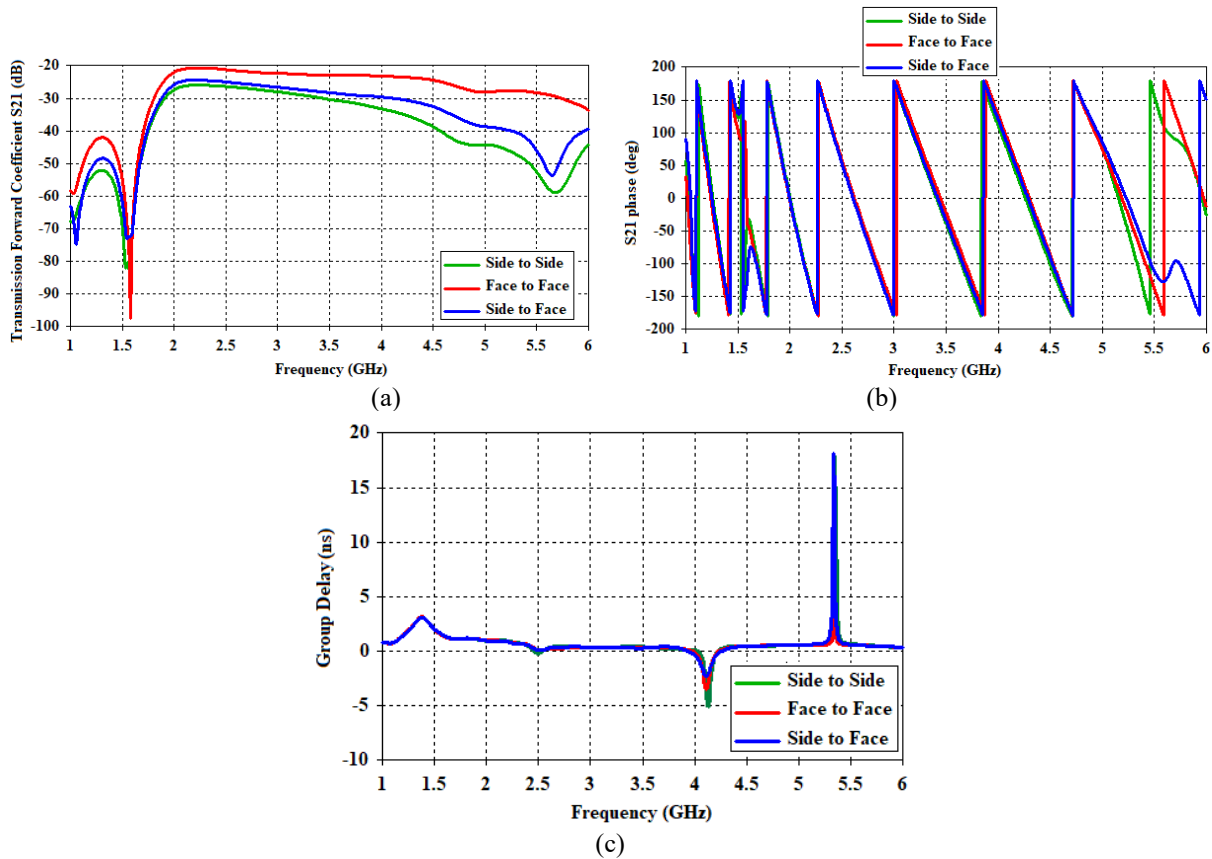


Fig. 11. Time Domain Performance Analysis of the suggested Antenna. (a) Transmission forward coefficient, (b) S21 phase, and (c) group delay.

5. Comparison with Related Works

It is difficult to give up small dimensions for a dual-band slot antenna with exceptional performance, despite efforts to create one with a low profile and better gain. This work presents a small, effective solution for a dual-band, wideband antenna-based DGS. The influence of human tissues and the dielectric back cover were studied since they are believed to be the most relevant in terms of mobile terminal applications. The suggested structure is created for WIFI and 5G applications.

The suggested dual-band slot antenna shows exceptional characteristics and performance in terms of size, fractional bandwidth (%), operating band (GHz), and gain (dBi) when compared to the works provided in the publications ranked #1 through #10 in Table 2. Table 2 lists the competing variants of the dual-band slot antenna designs that are available. These variations are displayed in the comparison. The findings clearly show that the suggested antenna, which is appropriate for 5G terminal devices, is smaller than the reference antennas when considering the size of the complete antenna, including the ground plane.

Table 2. Detailed comparison of the proposed dual-band slot antenna with the most recent research literature.

| No. # | Ref | Size | Fractional Bandwidth (%) | Operating Band (GHz) | Gain (dBi) |
|-------|----------------------|--------------------------------------|--------------------------|-------------------------------------|------------|
| 1 | (L. Dang 2010) | $0.46\lambda_0 \times 0.29\lambda_0$ | 23.2 | 2.3–3.0 3.25–3.68 4.9–6.2 | 4.32 |
| 2 | (M. Bod 2012) | $0.24\lambda_0 \times 0.18\lambda_0$ | N/A | 3.1–10.6 | 2.5 |
| 3 | (W. Hu 2011) | $0.38\lambda_0 \times 0.34\lambda_0$ | 25.7 | 2.34–2.82 3.16–4.06 4.69–5.37 | 3.02 |
| 4 | (R. Pandeewari 2018) | $0.9\lambda_0 \times 0.78\lambda_0$ | 67.5 | 2.75–5.45 | 8.4 |

| | | | | | |
|-----------------------------|----------------------|--------------------------------------|------|------------------------------------|------|
| 5 | (K.F. Lee 2008) | $0.39\lambda_0 \times 0.28\lambda_0$ | 33 | 3.5–3.75 4.85–5.2 5.5–5.7 | 8 |
| 6 | (I.R.R. Barani 2019) | $0.24\lambda_0 \times 0.19\lambda_0$ | 40 | 4.8–5.18 5.63–5.95 6.25–6.83 | 8 |
| 7 | (Q. Xue 2012) | $1.02\lambda_0 \times 1.31\lambda_0$ | 55 | 1.62–2.85 | 7.3 |
| 8 | (Y.M. Pan 2016) | $0.62\lambda_0 \times 0.62\lambda_0$ | 68 | 1.09–2.08 | 8.1 |
| 9 | (I. Ishteyaq 2021) | $0.82\lambda_0 \times 0.69\lambda_0$ | 28.4 | 4–6 | 8.2 |
| 10 | (J. Parsa 2023) | $0.3\lambda_0 \times 0.17\lambda_0$ | 60.6 | 3.29–3.63 4.39–5.2 | 7.17 |
| Proposed work 1 (dual band) | | $0.35\lambda_0 \times 0.35\lambda_0$ | 57.6 | 1.8–3.7 4.05–5.8 | 6.1 |
| Proposed work 2 (wide band) | | $0.35\lambda_0 \times 0.35\lambda_0$ | 60 | 2.05 – 5.8 | 6.1 |

Where λ_0 represents the free-space wavelength.

6. Conclusion

The innovative planar antenna based semicircular slot in ground plane with dual-band / wideband operation for WIFI and sub-6 GHz 5G wireless applications is the main interest of this article. The CST Microwave Studio software package has been used to simulate the proposed dual-band / wideband antenna design. The performance of the antenna with respect to its parameters was analyzed considering the 10 dB return loss $|S_{11}|$, peak gain (dBi), total efficiency, radiation patterns, and SAR value calculations. The stand-alone antenna without a back cover has a small footprint of $(0.35\lambda_0 \times 0.35\lambda_0)$, peak gain, and efficiency of about 8.5 dBi and 93%, respectively. This antenna's less complicated design, cheaper fabrication cost, and all the associated factors make it a potential candidate for 5G and sub-6 GHz WIFI applications.

Acknowledgements

The authors express their gratitude to the New Damietta Higher Institute of Engineering and Technology (NDETI), Damietta, Egypt, for their support in this project.

Disclosure

The authors declare no competing interests.

References

- U. Rafique, S. Khan, S. M. Abbas and P. Dalal. (2022). Uni-planar MIMO Antenna for Sub-6 GHz 5G Mobile Phone Applications. *2022 IEEE Wireless Antenna and Microwave Symposium (WAMS)*, Rourkela, Vol. 12, No. 8, pp. 1-5, doi: 10.1109/WAMS54719.2022.9848366.
- S. M. Asif, M. R. Anbiyaei, K. L. Ford, T. O'Farrell and R. J. Langley. (2019). Low-Profile Independently- and Concurrently-Tunable Quad-Band Antenna for Single Chain Sub-6GHz 5G New Radio Applications. *IEEE Access*, vol. 7, pp. 183770-183782, doi: 10.1109/ACCESS.2019.2960096.
- S. Sarkar, K. V. Srivastava. (2018). Four element dual-band sub-6 GHz 5G MIMO antenna using SRR-loaded slot-loops. *IEEE Uttar Pradesh section international conference on electrical, electronics and computer engineering (UPCON)*, pp. 1-5, doi: {10.1109/UPCON.2018.8596789.
- Elabd R.H., Abdullah H.H., Abdelazim M., talb A. abo, and shaban A. (2020). Low Complexity High- Performance Precoding Algorithms for mm-Wave MU-MIMO Commu-nication System", *Wirel. Pers. Commun.* (Springer). <https://doi.org/10.1007/s11277-020-07692-6>
- L. Dang, Z.Y. Lei, Y.J. Xie, G.L. Ning and J. Fan. (2010). A compact microstrip slot triple-band antenna for WLAN/WiMAX applications. *IEEE Antennas and Wireless Propagation Letters*, vol. 9, pp. 1178-1181, doi: 10.1109/LAWP.2010.2098433

- Z. Zhou, Z. Wei, Z. Tang and Y. Yin. (2019). Design and analysis of a wideband multiple-microstrip dipole antenna with high isolation. *IEEE Antennas and Wireless Propagation Letters*, vol. 18, no. 4, pp. 722-726, doi: 10.1109/LAWP.2019.2901838.
- Y. Liu, X. Li, L. Yang and Y. Liu. (2017). A dual-polarized dual-band antenna with omni-directional radiation patterns. *IEEE transactions on antennas and propagation*, vol. 65, no. 8, pp. 4259-4262, Aug. doi: 10.1109/TAP.2017.2708093.
- M. Li, Y. Ban, Z. Xu, G. Wu, C. Sim, K. Kang and Z. Yu. (2016). Eight-port orthogonally dual-polarized antenna array for 5G smartphone applications. *IEEE Transactions on Antennas and Propagation*, vol. 64, no. 9, pp. 3820-3830, 2016, doi: 10.1109/TAP.2016.2583501
- M. Bod, H.R. Hassani and M.S. Taheri. (2012). Compact UWB printed slot antenna with extra bluetooth, GSM, and GPS bands. *IEEE antennas and wireless propagation letters*, vol. 11, pp. 531-534, doi: 10.1109/LAWP.2012.2197849.
- W. Hu, Y. Yin, P. Fei and X. Yang. (2011). Compact triband square-slot antenna with symmetrical L-strips for WLAN/WiMAX applications. *IEEE Antennas and Wireless Propagation Letters*, vol. 10, pp. 462-465, doi: 10.1109/LAWP.2011.2154372.
- X. Dong, Z. Liao, J. Xu, Q. Cai and G. Liu. (2014). Multiband and wideband planar antenna for WLAN and WiMAX applications. *Progress in Electromagnetics Research Letters*, vol. 46, pp. 101-106, doi: 10.2528/PIERL14050103.
- W. Hu, X. Liu, S. Gao, L. Wen, L. Qian, T. Feng, R. Xu, P. Fei and Y. Liu. (2019) Dual-band ten-element MIMO array based on dual-mode IFAs for 5G terminal applications. *IEEE Access*, vol. 7, pp. 178476-178485, doi: 10.1109/ACCESS.2019.2958745.
- A.K. Gautam, L. Kumar, B.K. Kanaujia and K. Rambabu. (2016). Design of compact F-shaped slot triple-band antenna for WLAN/WiMAX applications. *IEEE Transactions on Antennas and Propagation*, vol. 64, no. 3, pp. 1101-1105, doi: 10.1109/TAP.2015.2513099.
- B. Huang, W. Lin, J. Huang, J. Zhang, G. Zhang and F. Wu (2019). A patch/dipole hybrid-mode antenna for sub-6GHz communication," *Sensors*, vol. 19, no. 6, pp. 1358. doi: 10.3390/s19061358.
- R. Pandeewari, "Complimentary split ring resonator inspired meandered CPW-fed monopole antenna for multiband operation. *Progress In Electromagnetics Research C*, vol. 80, pp.13-20, 2018, doi: 10.2528/PIERC17101402.
- H. Alsaif, M. Usman, M. Chughtai and J. Nasir. (2018). Cross polarized 2×2 UWB-MIMO antenna system for 5G wireless applications. *Progress In Electromagnetics Research M*, vol. 76, pp. 157-166. doi:10.2528/PIERM18101103.
- R. Khan, A.A. Al-Hadi, P.J. Soh, M. Ali, S. Al-Bawri and O. Owais. (2018). Design and optimization of a dual-band Sub-6 GHz four port mobile terminal antenna performance in the vicinity of user's hand. *Progress In Electromagnetics Research C*, vol. 85, pp. 141-153. doi: 10.2528/PIERC18050101.
- Elabd R. H., Abdullah H.H., Abdelazim M., A. abo talb, and A. shaban. (2019). Studying the Performance of Linear Precoding Algorithms based on Millimeterwave MIMO Communication System. *International Journal of Scientific and Engineering Research (IJSER)*, vol.10, no. 1, pp.2076-2082.
- W.C. Mok, S.H. Wong, K.M. Luk and K.F. Lee. (2013). Single-layer single-patch dual-band and triple-band patch antennas. *IEEE transactions on antennas and propagation*, vol. 61, no. 8, pp. 4341-4344. doi: 10.1109/TAP.2013.2260516.
- K.F. Lee, S.L.S. Yang and A.A. Kick. (2008). Dual-and multiband U-slot patch antennas. *IEEE Antennas and Wireless Propagation Letters*, vol. 7, pp. 645-647. doi: 10.1109/LAWP.2008.2010342.
- I.R.R. Barani, K. Wong, Y. Zhang and W. Li. (2019). Low-Profile Wideband Conjoined Open-Slot Antennas Fed by Grounded Coplanar Waveguides for 4×4 5G MIMO Operation," *IEEE Transactions on Antennas and Propagation*, vol. 68, no. 4, pp. 2646-2657. doi: 10.1109/TAP.2019.2957967.
- ANSI. (2006). Safety Levels with Respect to Human Exposure to Radio-Frequency Electromagnetic Fields, 3 kHz-300 GHz. *IEEE Std C*, vol. 95, no. 1.
- Ahlbom, U. Bergqvist, J. H. Bernhardt, J. P. Cesarini, M. Grandolfo, M. Hietanen and R. Matthes. (1998). Guidelines for limiting exposure to time-varying electric, magnetic, and electromagnetic fields (up to 300 GHz). *Health physics*, Vol. 74, No. 4, pp. 494-521. doi: 10.1097/00004032-199903000-00014.
- N.W. Liu, L. Zhu, W.W. Choi and J.D. Zhang. (2018). A low-profile differentially fed microstrip patch antenna with broad impedance bandwidth under triple-mode resonance. *IEEE Antennas and Wireless Propagation Letters*, vol. 17, no. 8, pp. 1478-1482. doi: 10.1109/LAWP.2018.2850045.
- Q. Xue, S.W. Liao and J.H. Xu. (2012). A differentially-driven dual-polarized magneto-electric dipole antenna. *IEEE transactions on antennas and propagation*, vol. 61, no. 1, pp. 425-430. doi: 10.1109/TAP.2012.2214998.

- Y.M. Pan, P.F. Hu, X.Y. Zhang and S.Y. Zheng. (2016). A low-profile high-gain and wideband filtering antenna with metasurface. *IEEE Transactions on Antennas and Propagation*, vol. 64, no. 5, pp. 2010-2016. doi: 10.1109/TAP.2016.2535498.
- I. Ishteyaq, I. S. Masoodi and K. Muzaffar. (2021). A compact double-band planar printed slot antenna for sub-6 GHz 5G wireless applications. *International Journal of Microwave and Wireless Technologies*, vol. 13, no. 5, pp. 469-477. doi: 10.1017/S1759078720001269.
- J. Parsa and A. Webb. (2023). Specific absorption rate (SAR) simulations for low-field. *Magma (New York, NY)*, vol. 36, no. 3, pp. 429-438. doi: 10.1007/s10334-023-01073-3.